Investigation of the Buffet Characteristics of Two Supercritical Airfoils

B. H. K. Lee,* F. A. Ellis,† and J. Bureau‡
National Research Council, Ottawa, Ontario, Canada

The buffet characteristics of two supercritical airfoils were investigated at the high Reynolds number two-dimensional test facility of the National Aeronautical Establishment. The design conditions of these two airfoils were quite similar. The thickness-to-chord ratio differed from each other by approximately 35%. The buffet onset boundaries were determined from the divergence of the unsteady balance normal force. They were compared to show the effect of thickness-to-chord ratio on buffet onset. One of the airfoils was instrumented with fast-response pressure transducers on the upper surface. Pressure intensities for shock-induced separation with reattachment as well as fully separated flows were measured. For flow conditions where discrete-frequency shock wave oscillations occurred, ensemble averaging of the unsteady pressure were carried out to determine the propagation of the pressure wave induced by periodic shock motion. Spectral analyzes of the pressure and normal force fluctuations were carried out quite deep into the buffet regime. Broadband convection velocities of the turbulent eddies were measured for fully separated flows.

Nomenclature

b = model span
C_L = lift coefficient from balance measurement
$C_{L_{max}}$ = maximum lift coefficient
C_{L_α} = local lift-curve slope
C_N = fluctuating normal-force coefficient from balance measurement
C_N' = rms value of normal-force coefficient
C_p = pressure coefficient, p/q_∞
C_{p_s} = steady-state pressure coefficient
$C_{p'}$ = rms value of pressure coefficient
$\tilde{C}_p$ = oscillatory pressure coefficient, from periodic shock motion
$\bar{C}_p$ = ensemble averaged pressure coefficient, $C_{p_s} + \tilde{C}_p$
c = chord length
M = Mach number
N_{rms} = rms value of normal force from balance measurement
p = instantaneous pressure
p_{rms} = rms value of unsteady pressure
q_∞ = freestream dynamic pressure
$R(a,b,\tau)$ = cross correlation of functions a and b
U_∞ = freestream velocity
x = distance measured in flow direction from airfoil leading edge
α = angle of incidence
ϕ = phase angle in degree
τ = time delay

Introduction

INVESTIGATIONS of supercritical airfoils at the National Aeronautical Establishment (NAE) have shown that they possess favorable buffet characteristics compared with conventional airfoils. A number of recent studies[1-3] provided important physical insight into the characteristics of buffeting flows. Because of the complexities of the buffet phenomenon, most of the existing methods[4-7] on estimating buffet loads relied on experimental data derived from wing-tunnel tests. This is especially true for supercritical airfoils. Further investigations are needed to give a better understanding of transonic shock-boundary-layer interactions and associated oscillatory shock motions so that a better model describing wing buffeting can be formulated.

Two supercritical airfoils were recently investigated at the NAE high Reynolds number two-dimensional test facility.[8] The design conditions of the airfoils were quite similar. The thickness-to-chord ratio differed from each other by approximately 35%. This paper describes some of the techniques used in this study and presents results that are useful to the understanding of the phenomenon of wing buffeting at transonic flows. Buffet intensities were determined from the balance normal-force measurements, and buffet onset boundaries were derived from the divergence of the fluctuating normal force. For flow conditions where buffet onset was primarily due to trailing-edge separation, this technique[9] was shown to give results in good agreement with those determined from the criterion using the trailing-edge pressure divergence.[10] The effect of airfoil thickness on buffet onset was studied and comparisons of the buffet boundaries for these two airfoils are given.

Investigations of unsteady pressure fluctuations were carried out using fast-response transducers flush mounted on the upper surface of one of the airfoils. At various degrees of buffet severity, the types of shock boundary-layer interaction were identified from steady and unsteady pressure measurements. The pressure waves generated by the periodic shock motion were detected by ensemble averaging of the pressure-transducer outputs. Spectral analyzes of the surface pressures and normal forces were carried out quite deep inside the buffet regime. At these conditions, the flow was fully separated. Cross correlation of the pressure field was carried out to determine the broadband convection velocities of the turbulent eddies.

Models, Instrumentation, and Data Processing

The first airfoil investigated was designed by deHavilland Aircraft Company of Canada and designated as WTEA II. The airfoil was used in a previous joint NAE-deHavilland research and development program aimed at improvements in design that would reduce wing-section drag. The design condi-

Received June 4, 1988; revision received Feb. 1, 1989.

*Senior Research Officer, High-Speed Aerodynamics Laboratory, National Aeronautical Establishment. Member AIAA.

†Research Council Officer, High-Speed Aerodynamics Laboratory, National Aeronautical Establishment.

‡Technical Officer, High-Speed Aerodynamics Laboratory, National Aeronautical Establishment.

tions were for a cruise Mach number of 0.72 and a lift coefficient of 0.6. The detailed profile of the airfoil is given in Ref. 9. It was made of aluminum with 12-in. chord and a 15-in. span. The maximum thickness-to-chord ratio was 16%. The original airfoil was modified in the studies carried out in Ref. 9 by the addition of a flap. The length of the flap was approximately 14% chord and the trailing-edge thickness was 0.1% chord. The flap angle was set at 0 deg for this investigation. There were 79 pressure orifices on the model surface for static pressure measurements; 43 of them were located on the airfoil upper surface and 23 on the lower surface. There were 13 pressure orifices on the flap with six on either surface and one at the trailing edge.

The second model tested was the Bauer-Garabedian-Korn (BGK) No. 1 airfoil.[2] The chord of the airfoil was 10 in. and the span was 15 in. The thickness-to-chord ratio was 11.8%. A detailed sketch of the profile and locations of orifices for static pressure measurements is given in Ref. 11. There were 50 pressure orifices on the upper surface and 20 on the lower surface. The design M and C_L were 0.75 and 0.63, respectively. A modification to the original airfoil was made and involved milling off a 0.75-in. wide, 8-in. long groove from the upper surface, 2.5 in. from the centerline. A replacement insert was made and 16 25-psid miniature Kulite differential pressure transducers with a 0.062-in. diam were installed. The locations of the transducers are shown on the top of Fig. 6. The second transducer F, located at 2.5 in. from the airfoil leading edge, was defective and was not used in the tests. The intensities of the fluctuating pressure are expressed in coefficient form as

$$C_p' = p_{\text{rms}}/q_\infty \tag{1}$$

The lift and pitching moment of the airfoil were determined by use of a side-wall balance. In addition to the steady-state values of the balance force, the fluctuating components were also measured. The rms values of the normal force are presented in coefficient form by

$$C_N' = N_{\text{rms}}/q_\infty b\, c \tag{2}$$

Spectral analyses of the transducers and balance outputs were performed. The signals were sampled at 1.6 kHz and analyzed digitally on a computer using the IEEE routine PMPSE[12] to give power spectra. A fast Fourier transform (FFT) block size of 256 and a signal duration of 2 s were chosen for the analyzes. For cross-correlation studies, the IEEE routine CMPSE[12] was used. The pressure signals were recorded on an FM tape recorder at 60 in./s and analyzed at a reduced speed of 3.75 in./s. Sampling speed was also 1.6 kHz and an FFT block size of 1024 was used. Signal durations of approximately 10 s were analyzed.

The force balance was very stiff and both the lowest frequencies of rigid-body airfoil heave and fixed-fixed wing bending were much larger than the peak excitation frequencies observed under buffet conditions. These frequencies were due to shock oscillations and increased from approximately 50 Hz at $M=0.612$ to 80 Hz at $M=0.792$ for the WTEA II airfoil. For the BGK No. 1 airfoil, the buffet excitation frequencies were 70–80 Hz for M between 0.688 and 0.796. In wind-off tests, the balance with the WTEA II airfoil installed was subjected to impulse excitation. The response was measured and four natural frequencies were detected at 140, 215, 320, and 360 Hz. They were all greater than the buffet excitation frequencies. No wind-off tests were conducted using the BGK No. 1 airfoil, but the force-balance characteristics should be similar to the WTEA II tests.

A fast-response pressure transducer was installed on the side wall of the wind tunnel during the BGK No. 1 airfoil tests to measure the unsteady tunnel pressure. It was located approximately 26 in. upstream of the airfoil leading edge. A discrete frequency of approximately 420 Hz was detected. The magnitude of this pressure oscillation depended on M and α of the airfoil. The origin of this flow disturbance so far has not been identified from the NAE wind tunnel.

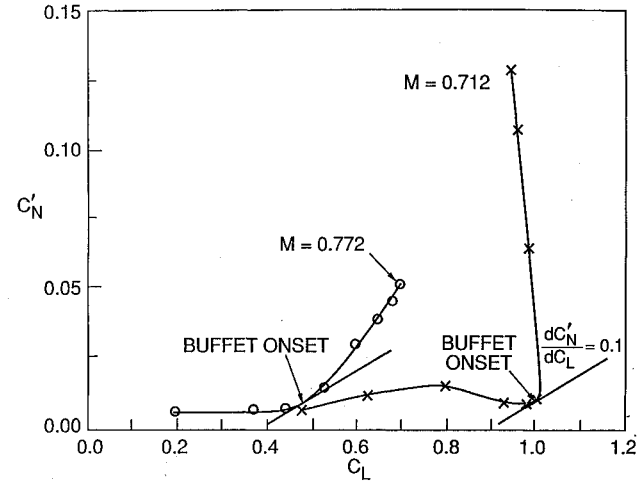

Fig. 1 Normal-force fluctuations vs lift coefficients for WTEA II airfoil.

Distributed suction was applied through porous plates to regions of the tunnel side walls in the vicinity of the model. The amount of suction was selected so as to minimize any three-dimensional effects.[8] The tests were performed at chord Reynolds number of 20×10^6 for both airfoils with free transition on the models. At design conditions, flow visualization on the WTEA II airfoil using a thin film of oil containing a dye, which fluoresced in ultraviolet light, showed transition to occur on the upper surface at less than 5% chord from the leading edge. For the BGK No. 1 airfoil, previous tests have estimated transition to be in the neighborhood of 10% chord from the leading edge. The Mach number in this investigation varied between 0.612 and 0.792 for the WTEA II and between 0.5 and 0.818 for the BGK No. 1 airfoil.

Results and Discussion

Buffet Boundaries

The rms values of the normal-force fluctuations C_N' are plotted vs C_L in Fig. 1 for the WTEA II airfoil. For supercritical airfoils, the curve for $M=0.712$ is typical of the behavior of C_N' with C_L when a $C_{L_{\max}}$ in the lift vs α curve is present. At higher M, usually a $C_{L_{\max}}$ is not observed even when α far exceeded the buffet onset value. The C_N' vary with C_L in a manner shown by the curve for $M=0.772$. To determine the C_L at buffet onset, the procedure is to obtain a smooth C_N' vs C_L curve either by the use of a spline or fitting manually. C_L at buffet is then determined by noting the point on the curve with a slope of $dC_N'/dC_L=0.1$. This value is arbitrarily chosen. When buffet onset is primarily due to trailing-edge separation, the results are found to be consistent with those derived using the trailing-edge pressure divergence criterion. This has been demonstrated in Ref. 9 where the values of α at buffet onset determined from both methods were found to be very close. Instead of C_L, α is sometimes used to define the buffet onset boundary. In this case, α is determined from the C_N' vs α curve at a point where the slope is

$$dC_N'/d\alpha = 0.1\, C_{L_\alpha} \tag{3}$$

Experience at NAE in testing supercritical airfoils shows that it is more convenient to use the fluctuating normal force from a balance to determine buffet onset. Installation of a pressure orifice close to or at the trailing edge to measure pressure divergence is cumbersome and often not feasible for airfoils with thin trailing edge. Also, it is often necessary to obtain trailing-edge pressure data over a wide range of incidence

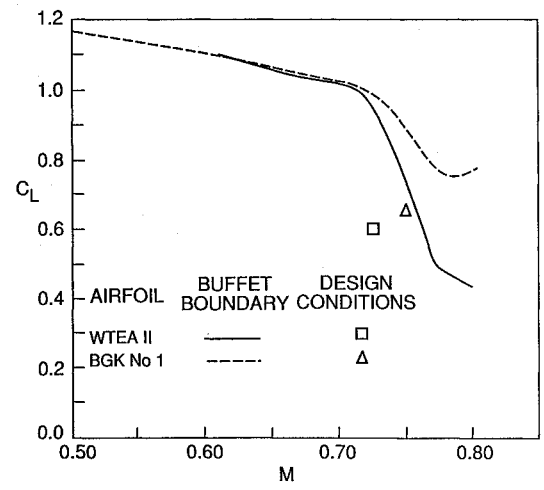

Fig. 2 Buffet boundaries for WTEA II and BGK No. 1 airfoils.

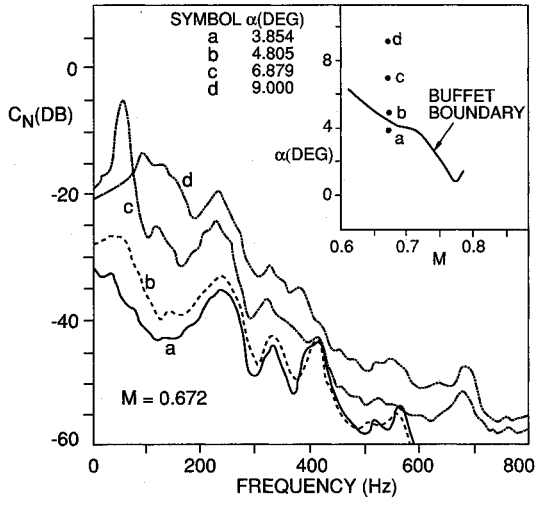

Fig. 3 Variations of normal-force power spectra with α at $M=0.672$ for WTEA II airfoil.

below buffet onset in order to define a baseline to locate α when trailing-edge pressure divergence occurs.

Figure 2 shows the buffet boundaries for the WTEA II and BGK No. 1 airfoils. For $M<0.71$, the two boundaries are very close and nearly coincide with each other. When M exceeds 0.71, the WTEA II airfoil shows buffet to occur at C_L smaller than those for the thinner BGK No. 1 airfoil. The differences in buffet onset C_L are quite large at the higher values of M. Increasing the airfoil thickness usually results in larger unsteady normal forces detected inside the buffet regime.

Power Spectra of Normal Forces from Balance Measurements

Figures 3 and 4 show the effect of varying α on the normal-force power spectra at $M=0.672$ and 0.752, respectively, for the WTEA II airfoil. On the upper right-hand corner of the figures, the buffet boundary (α vs M) is plotted for reference. The peaks in these figures at approximately 140, 215, 320, and 360 Hz correspond to the natural frequencies of the force balance.[9] The disturbance at 420 Hz is from the wind tunnel. The peaks having frequencies of 55 Hz at $M=0.672$ and 75 Hz at $M=0.752$ are from shock wave oscillations on the upper surface of the airfoil. In a study[13] on the periodic shock motion caused by transonic-shock boundary-layer interaction, a model for the self-sustained shock oscillations was proposed. The propagation velocity of the pressure disturbance due to the shock motion was measured experimentally for the BGK No. 1 airfoil. Using this velocity, the oscillating shock frequencies were calculated. They were found to be close to the measured values of 70–80 Hz for M between 0.688 and 0.746. The shock oscillation frequencies for the WTEA II airfoil

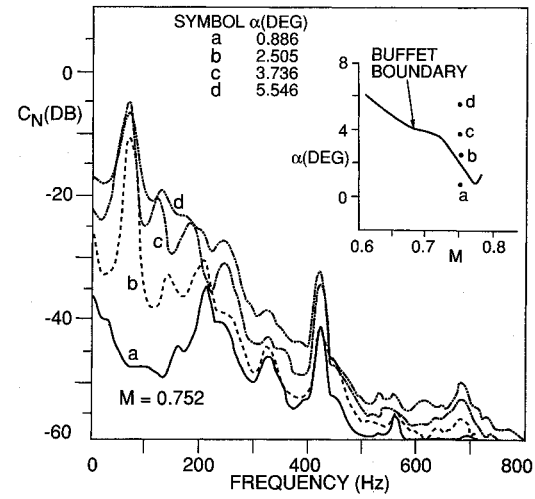

Fig. 4 Variations of normal-force power spectra with α at $M=0.752$ for WTEA II airfoil.

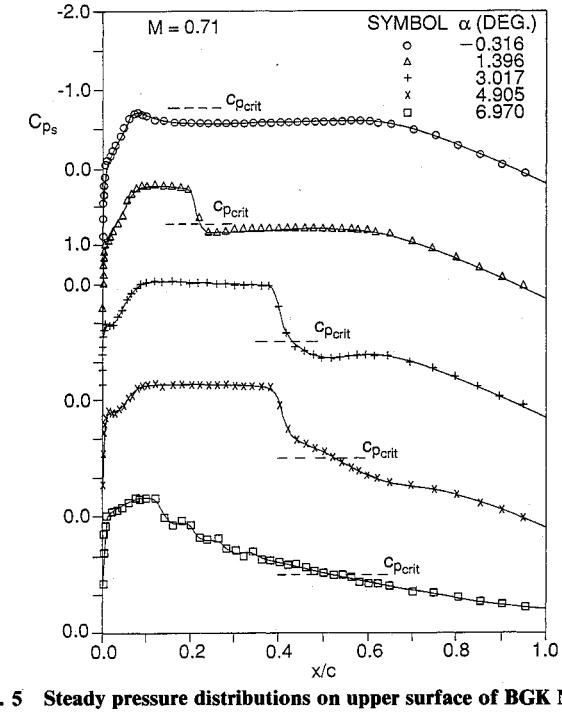

Fig. 5 Steady pressure distributions on upper surface of BGK No. 1 airfoil at various α.

derived from normal-force spectra are 50–80 Hz for M between 0.612 and 0.792.

Beyond the buffet onset boundary, the shock wave strengthens as α is increased. For a given M, there is a maximum α above which the shock starts to weaken and a periodic shock motion is not detected. At $M=0.672$ and $\alpha=9$ deg, it can be seen from the normal-force spectra shown in Fig. 3 that the shock has weakened considerably. A slight decrease in the shock strength is noticeable in Fig. 4 at $M=0.752$ and $\alpha=5.546$ deg. The WTEA II airfoil was not tested at sufficiently large α to show the region in the α vs M plot where discrete shock oscillations ceased to exist. However, results for the BGK No. 1 airfoil illustrating this behavior of shock wave oscillation with α is given in Ref. 13.

Pressure Measurements on Airfoil Upper Surface

Figures 5 and 6 show results for the steady and unsteady pressure distributions on the upper surface of the BKG No. 1 airfoil at $M=0.71$. At $\alpha=-0.316$ deg, Fig. 5 shows the flow on the upper surface to be subcritical. The corresponding C_p' (Fig. 6) is quite small and reverts to the value measured by the wind-tunnel side-wall transducer designated as "tunnel level"

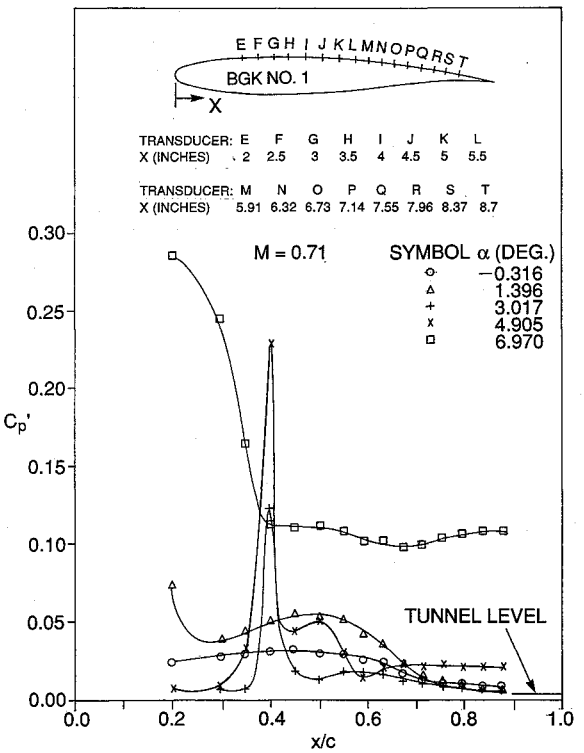

Fig. 6 Variations of pressure intensities on upper surface of BGK No. 1 airfoil at various α.

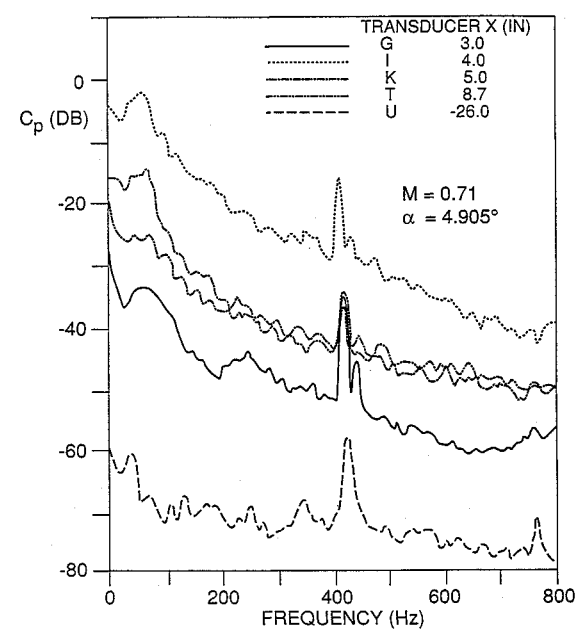

Fig. 7 Power spectra of unsteady pressure on upper surface of BGK No. 1 airfoil at $M=0.71$ and $\alpha=4.905$ deg.

as the trailing edge is approached. At $\alpha=1.396$ deg, a weak shock is formed and the turbulent boundary layer thickens near the interaction region but without separating. There is a small increase in pressure intensity behind the shock. Increasing α to 3.017 deg results in a large rise in C_p' behind the shock at $x/c=0.4$. The fluctuating pressure is limited to a small region near the shock. For the three values of α considered so far, C_p' at the last measuring position are very close to the tunnel level. This indicates that trailing-edge separation has not occurred, or at least it has not reached the position of the last pressure transducer at $x/c=0.87$. The normal-force spectra do not show any peaks in the neighborhood of 75 Hz, thus indicating the absence of any noticeable shock oscillations.

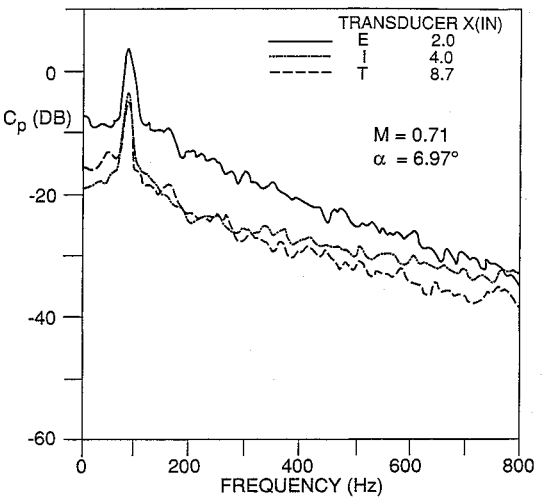

Fig. 8 Power spectra of unsteady pressure on upper surface of BGK No. 1 airfoil at $M=0.71$ and $\alpha=6.97$ deg.

At $\alpha=4.905$ deg, the steady pressure results show the formation of a stronger shock, which causes the flow to separate and reattaches to form a bubble. The intensities of the pressure fluctuations are practically constant in the reattached region, which starts from x/c approximately 0.6 and continues to the last measuring point at $x/c=0.87$. Rather than terminating at the last transducer location, this region probably extends further downstream towards the trailing edge. C_p' measured at the last transducer is slightly higher than the tunnel level. The steady-state C_{p_s} distributions show a small "hump" at x/c between 0.45 to 0.6. This "hump" in the steady-state pressure distribution is usually attributed to a separation bubble. The large "bulge" in the C_p' distributions shown in Fig. 6 is more accurate in determining the dimensions of the separation bubble behind the shock. The peak pressure intensity inside the bubble is located at x/c approximately 0.5.

When α is increased to 6.97 deg, the flow becomes fully separated. The pressure intensities are large behind the shock but decrease rapidly and reach a nearly constant value of about 0.1 from $x/c=0.4$ to 0.87. This value of C_p' is significantly higher than the tunnel level of 0.004. This value of the tunnel intensity is an average value at $M=0.71$ for α between -0.316 and 6.97 deg.

The pressure power spectra are shown in Fig. 7 at $\alpha=4.905$ deg for the G, I, K and T tranducers. These locations are chosen to illustrate the behavior of the pressure fluctuations in the regions of interest associated with shock boundary-layer interaction. At transducer G upstream of the shock, the pressure level is usually very low and close to the tunnel level. Behind the shock (transducer I), there is a large increase in pressure fluctuations over a wide frequency range. In this study, the highest frequency used in computing the spectra is 800 Hz. A broad peak at about 75 Hz is observed in the pressure spectra for transducer I and K. This is due to the presence of a weak oscillating shock wave. The pressure field decays very rapidly and the magnitude is very small at transducer location M, as shown in Fig. 6. There are some noticeable differences in the spectra between transducers K and T in the low-frequency range below 200 Hz. The spectra for transducers M to S, which are not shown here, are very similar to that at T closest to the trailing edge. The spectra for transducer U, located 26 in. upstream of the airfoil leading edge, is included in the figure to show the tunnel-wall pressure fluctuations. The vertical scale is displaced 20 db downwards in Fig. 7 to avoid overlapping with the T transducer spectra. The 420-Hz peak is very dominant.

At $\alpha=6.97$ deg, the flow is fully separated. The pressure power spectra for transducers E, I, and T are shown in Fig. 8. The large peaks at approximately 75 Hz are due to strong

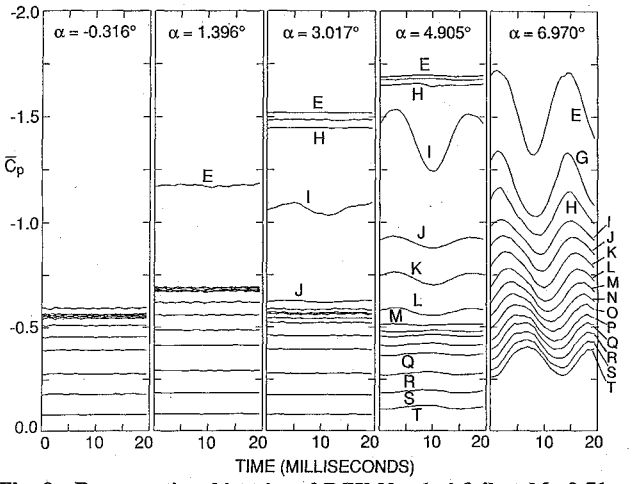

Fig. 9 Pressure-time histories of BGK No. 1 airfoil at $M=0.71$.

shock oscillations. The pressure power spectra for transducers I to T are very similar.

Pressure-Time Histories Due to Shock Oscillations

The unsteady pressure fluctuations behind the periodic shock wave have contributions from two sources; namely, a random component associated with the turbulent motion in the separated flow region and a deterministic part ($\tilde{C}_p$) from the pressure field as a result of shock wave oscillation. The magnitude of $\tilde{C}_p$ is usually small compared to that from turbulent fluctuations. To determine the oscillatory pressure wave component, the periodic shock frequency was first obtained from the balance normal-force spectra. The balance output was then passed through a bandpass filter. The bandwidth was 20 Hz and the center frequency corresponded to the shock oscillation frequency. The zero crossings of the filtered balance signal were detected. Approximately 175 ensemble averages of the pressure signals were performed. Each ensemble, which was synchronized to the zero crossings, had 32 samples. A Fourier analysis was then performed on the ensemble-averaged $\tilde{C}_p$ time histories to obtain the fundamental and harmonics of the oscillatory pressure field.

In Fig. 9, the ensemble-averaged $\tilde{C}_p$ time histories are shown for $M=0.71$ and the values of α are the same as those used to obtain Figs. 5 and 6. At $\alpha=-0.316$ deg, Fig. 5 shows the flow to be subcritical. At $\alpha=1.396$ deg, the shock is weak and the pressure fluctuations are very small, as indicated in Fig. 6. The $\tilde{C}_p$ time histories for these two values of α are practically lines of constant magnitude having the steady-state C_{p_s} values. At $\alpha=3.017$ deg, small pressure oscillations are observed at transducer I. The pressure field decays rapidly and fluctuations are hardly noticeable at transducer J, which is only 0.5 in. away. As α is increased to 4.905 deg, large pressure oscillations at transducer I are detected. Inside the separation bubble, the pressure fluctuations are quite uniform as shown in the $\tilde{C}_p$ traces for transducers J, K, and L. At transducer location M, which corresponds to the last point of the "bulge" in the C_p' curve shown in Fig. 6, the pressure fluctuations are very small. Downstream of transducer M, the pressure field shows a small growth in amplitude for decreasing distances from the trailing edge. For fully separated flows ($\alpha=6.97$ deg), the first transducer is behind the shock wave. The pressure amplitude decreases up to the position where transducer I is located. From then onwards, the pressure oscillates with a nearly constant amplitude as far as the last measuring point at $x/c=0.87$.

The magnitudes of the fundamental component of $\tilde{C}_p$ obtained from Fourier analysis of the ensemble averaged $\tilde{C}_p$ are shown in Fig. 10 for $\alpha=3.017$, 4.905, and 6.907 deg. The higher harmonics are quite small and are not considered in this paper. The corresponding phase angles are given in Fig. 11. It is seen at $\alpha=3.017$ deg the pressure fluctuations behind the

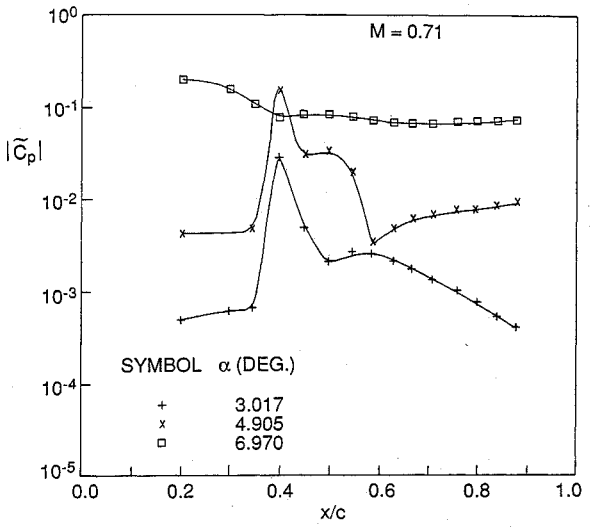

Fig. 10 Magnitude of pressure wave propagating downstream of the shock at $M=0.71$ and various α.

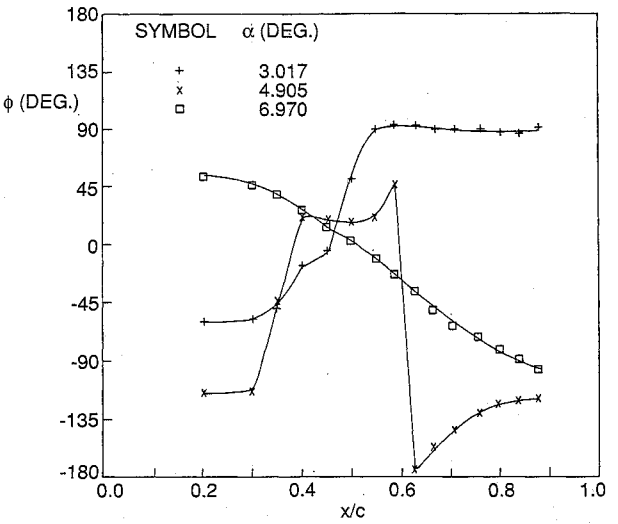

Fig. 11 Phase angle of pressure wave propagating downstream of the shock at $M=0.71$ and various α.

shock decay rapidly. From transducer K onwards, there is a more gradual decrease towards the trailing edge. In this slowly decaying pressure field, the phase angles remain practically unchanged. This indicates the whole region to be oscillating in phase. At $\alpha=4.905$ deg, there is a sharp phase change across the shock. In the separated flow region, the phase angles for transducers I to L are nearly constant. There is a sharp jump in phase across the reattachment point. This is followed by a gradual phase increase towards the trailing edge.

For fully separated flow, the phase variation downstream of the shock is quite linear and an average pressure wave propagation velocity can be computed. For the particular example given in the figure, the pressure wave velocity due to the shock oscillation is $0.12\ U_\infty$.

Ensemble-Averaged Pressure Distributions

The ensemble-averaged $\tilde{C}_p$ distributions at different phase angles during a shock oscillation cycle are shown in Fig. 12 for the BGK No. 1 airfoil at $M=0.732$ and $\alpha=6.05$ deg. Superimposed on these results are the time-averaged C_p obtained from the fast-response transducers using a signal duration of 2 s. Also shown in Fig. 12 are the pressure distributions obtained from scanivalve measurements. The duration of each scan is approximately 2.5 s and the results are the average of 5 scans. For the flow conditions used to obtain Fig. 12, the pressure fluctuations are large. The mean pressure distributions from

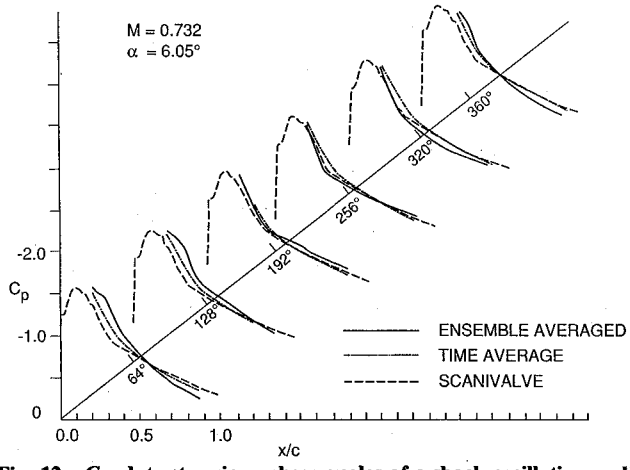

Fig. 12 C_p plots at various phase angles of a shock oscillation cycle for BGK No. 1 airfoil at $M=0.732$ and $\alpha=6.05$ deg.

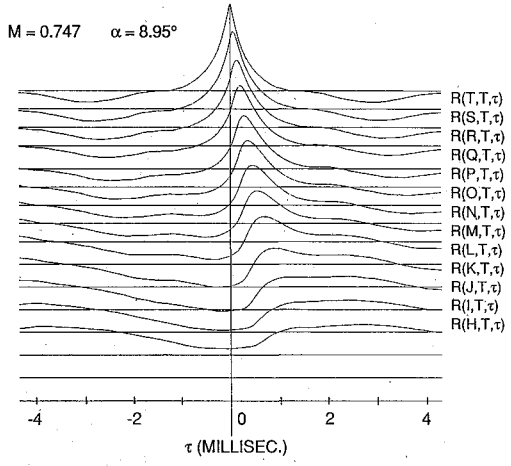

Fig. 13 Cross-correlation functions of pressure field for BGK No. 1 airfoil at $M=0.747$ and $\alpha=8.95$ deg.

scanivalve measurements are not accurate unless a large number of scans are averaged. This requires a testing duration longer than that available from the NAE high Reynolds number two-dimensional test facility. The amplitude of shock oscillation from the ensemble-averaged $\bar{C}_p$ data is quite large. The frequency of oscillation measured from the peak in the normal-force spectra is about 75 Hz.

Broadband Convection Velocities of Turbulent Eddies

To determine the convection velocities of the turbulent eddies in fully separated flows, cross correlation of the pressure signals was performed and analyzed digitally using the IEEE routine CMPSE.[12] An example is given in Fig. 13 for $M=0.747$ and $\alpha=8.95$ deg. The results are for the BGK No. 1 airfoil using the last transducer T signal as the reference. Knowing the separation distance between the transducers and the time delay τ for the peaks of the cross-correlation functions to pass over them, the convection velocity can be calculated. The broadband convection velocity derived from this figure is $0.552\ U_\infty$. It can be seen that the pressure remains coherent for quite large distances from the last transducer located at $x/c=0.87$. The results of this study show the broadband convection velocity to be dependent on M and α. At $M=0.747$ but lowering α to 4.55 deg, a convection velocity of $0.84\ U_\infty$ was obtained. No narrow-band cross correlation was carried out and, hence, comparisons with related studies[1] are not possible.

Conclusions

1) The onset of buffet can be determined quite accurately from plots of C_N' vs C_L at a value of C_L where the slope of the curve is 0.1. In the low M range, the buffet boundaries for the two airfoils tested are very close and nearly coincide with each other. When M is greater than its design value, a much more rapid decrease in C_L at buffet with M is observed for the thicker airfoil.

2) Inside the buffet regime, spectral analyzes of the balance normal-force outputs show shock oscillations of about 70–80 Hz for the BGK No. 1 airfoil at M between 0.688 and 0.796. For the WTEA II airfoils, the frequency range is between 50–80 Hz for $M=0.612$ to 0.792. The magnitudes of the fluctuating normal force have quite large values near the "elbow" of the buffet onset boundaries. As the Mach number increases, the normal-force fluctuations decrease and the shock waves become more steady.

3) Unsteady pressure measurements show the intensities of pressure fluctuations to be largest behind the shock. For fully separated flows, large-amplitude shock oscillations occur. A periodic pressure field is generated and propagates downstream from the shock wave. Depending on the flow conditions, the pressure amplitude either remains constant or decays slowly towards the trailing edge. A fairly linear variation in phase angle is detected. The pressure wave propagation velocity is small compared to the speed of acoustic waves. It is usually in the neighborhood of 10% of the freestream velocity.

4) The ensemble-averaged $\bar{C}_p$ distributions obtained at different phase angles of a shock oscillation cycle are useful in defining the position and amplitude of the shock wave during buffeting.

References

[1]Roos, F. W., "Some Features of the Unsteady Pressure Field in Transonic Airfoil Buffeting," *Journal of Aircraft*, Vol. 17, Nov. 1980, pp. 781–788.

[2]Lee, B. H. K. and Ohman, L. H., "Unsteady Pressures and Forces During Transonic Buffeting of a Supercritical Airfoil," *Journal of Aircraft*, Vol. 21, June 1984, pp. 439–441.

[3]Benoit, B. and Legrain, I., "Buffeting Prediction for Transport Aircraft Applications Based on Unsteady Pressure Measurements," AIAA Paper 87-2356, Aug. 1987.

[4]Lee, B. H. K., "A Method for Predicting Wing Response to Buffet Loads," *Journal of Aircraft*, Vol. 21, Jan. 1984, pp. 85–87.

[5]Lemley, C. E. and Mullans, R. E., "Buffeting Pressures on a Swept Wing in Transonic Flight—Comparison of Model and Full-Scale Measurements," AIAA Paper 73-311, March 1973.

[6]Butler, G. F. and Spavins, G. R., "Preliminary Evaluation of a Technique for Predicting Buffet Loads in Flight from Wind-Tunnel Measurements on Models of Conventional Construction," Paper No. 23, AGARD CP-204, Prediction of Aerodynamic Loading, 1976.

[7]Mabey, D. G., "Prediction of the Severity of Buffeting," Paper No. 7, AGARD-LS-94, Three-Dimensional and Unsteady Separation at High Reynolds Numbers, 1978.

[8]Ohman, L. H., "The NAE High Reynolds Number 15″ × 60″ Two-Dimensional Test Facility," National Research Council of Canada, NAE-LTR-HA-4, Pt. I, April 1970.

[9]Lee, B. H. K. and Tang, F. C., "Transonic Buffet of a Supercritical Airfoil and Trailing-Edge Flap," *Journal of Aircraft*, Vol. 26, May 1989, pp. 459–464.

[10]Pearcy, H. H., Osborne, J., and Haines, A. B., "The Interaction Between Local Effects at the Shock and Rear Separation—A Source of Significant Scale Effects in Wind-Tunnel Tests in Airfoils and Wings," Paper 11, AGARD CP 35, Transonic Aerodynamics, 1968.

[11]Lee, B. H. K. and Ohman, L., "Unsteady Pressure and Force Measurements Associated with Transonic Buffeting of a Two-Dimensional Supercritical Airfoil," National Research Council of Canada, NAE-AN-14, June, 1983.

[12]Rabiner, L. R., Schafer, R. W., and Dlugos, D., "Chapter 2.1: Periodgram Method for Power Spectrum Analysis," and "Chapter 2.2: Correlation Method for Power Spectrum Estimation," *Programs for Digital Signal Processing*, edited by the Digital Signal Processing Committe, IEEE Acoustics, Speech and Signal Processing Society, IEEE Press, New York, 1979.

[13]Lee, B. H. K., "Oscillatory Shock Motion Caused by Transonic Shock-Boundary-Layer Interaction," *AIAA Journal*, (to be published).